JCTC Journal of Chemical Theory and Computation

Article

pubs.acs.org/JCTC

Glucose-Promoted Localization Dynamics of Excess Electrons in Aqueous Glucose Solution Revealed by Ab Initio Molecular Dynamics Simulation

Jinxiang Liu,[†] Robert I. Cukier,[‡] Yuxiang Bu,*[,†] and Yuan Shang[§]

[†]Institute of Theoretical Chemistry, School of Chemistry and Chemical Engineering, Shandong University, Jinan, 250100, China

[‡]Department of Chemistry, Michigan State University, East Lansing, 48224-1322, United States

[§]National Supercomputer Center in Jinan, Jinan, 250101, China

Supporting Information

ABSTRACT: Ab initio molecular dynamics simulations reveal that an excess electron (EE) can be more efficiently localized as a cavity-shaped state in aqueous glucose solution (AGS) than in water. Compared with that (~1.5 ps) in water, the localization time is shortened by ~0.7−1.2 ps in three AGSs (0.56, 1.12, and 2.87 M). Although the radii of gyration of the solvated EEs are all close to 2.6 Å in the four solutions, the solvated EE cavities in the AGSs become more compact and can localize ~80% of an EE, which is considerably larger than that (~40−60% and occasionally ~80%) in water. These observations are attributed to a modification of the hydrogen-bonded network by the introduction of glucose molecules into water. The water acts as a promoter and stabilizer, by forming voids around glucose molecules and, in this fashion, favoring the localization of an EE with high efficiency. This study provides important information about EEs in physiological AGSs and suggests a new strategy to efficiently localize an EE in a stable cavity for further exploration of biological function.

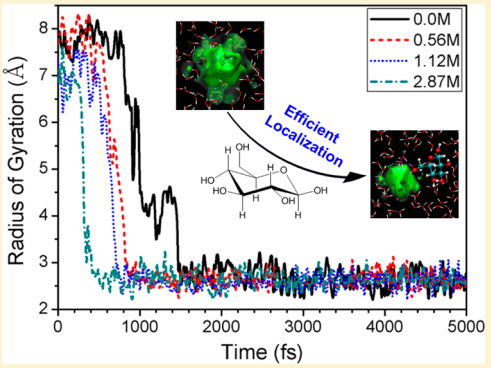

1. INTRODUCTION

The structures, states, and dynamics of an excess electron (EE) in melts, glasses, liquids, solutions, and even large clusters are difficult to characterize because of bulk effects and the role of thermal fluctuations in liquids and solutions.[1−8] Hydrated electrons have been characterized in liquid water as mainly localized, interior cavity-shaped solvated and in water clusters as mainly surface-bound Rydberg states.[1−8] In contrast to hydrated electrons in anionic clusters or solids, an EE in a fluid may exist in a plethora of states, ranging from cavity-shaped localized to completely diffuse states.[4−8] These states can interconvert (localized ↔ diffuse, and even compact cavity ↔ loose cavity), as driven by solvent fluctuations, and thus exhibit intriguing dynamics.[4−8] Many studies and experiments have demonstrated that solvated EEs can exist in highly stable localized states, in both molecular clusters and solutions, and they exhibit many desirable properties with potential applications.[9−24] EEs even can be used to detect solid defects via opto-acoustic techniques.[23,24] In addition, solvation of radiation-generated EEs can retard their damage to DNA and other biological species.[14,25] Clearly, it is of great interest to design strategies to enhance the efficiency of localization and solvation of EEs in fluid media.

The structure of a localized hydrated EE in water has recently been the subject of lively debates.[26−28] Localization of an EE in liquid water could be considerably different from that in water clusters due to the size effect of the clusters, although a large cluster similar to a liquid droplet can exhibit the bulk character well. This difference in localization can be attributed to their different H-bond networks, which controls how water molecules rearrange to free some dangling −OH hydrogens for binding an EE, or for forming a cavity for the EE to reside in. Thus, it is a challenging topic to find promising aqueous media for localizing EEs efficiently and promoting their stably solvated forms.

Inspired by the structure of glucose, aqueous glucose solutions (AGSs) should be promising media to reach this goal. Glucose is a typical representative of monosaccharides, the major building blocks for many important carbohydrate systems.[29,30] In solution, D-glucose exists in the pyranose form, and its five −OH groups are linked to five sites of the pyrane ring, with rotational freedom, thus offering the possibility of providing a cooperative set of potential EE-binding sites, as observed experimentally for intermolecularly trapped EEs in glucose crystals.[31−35] More importantly, glucose not only contains a hydrophobic backbone but also possess more hydrophilic −OH groups. Also, the viscosity of an AGS rises with increasing glucose content,[36] which leads to a decrease of water mobility. In addition, an isolated glucose molecule cannot form a stable molecular anion because its σ^* orbital is energetically too high for EE occupancy.[37] All these

Received: March 20, 2014
Published: August 23, 2014

   dx.doi.org/10.1021/ct500238k | J. Chem. Theory Comput. 2014, 10, 4189−4197

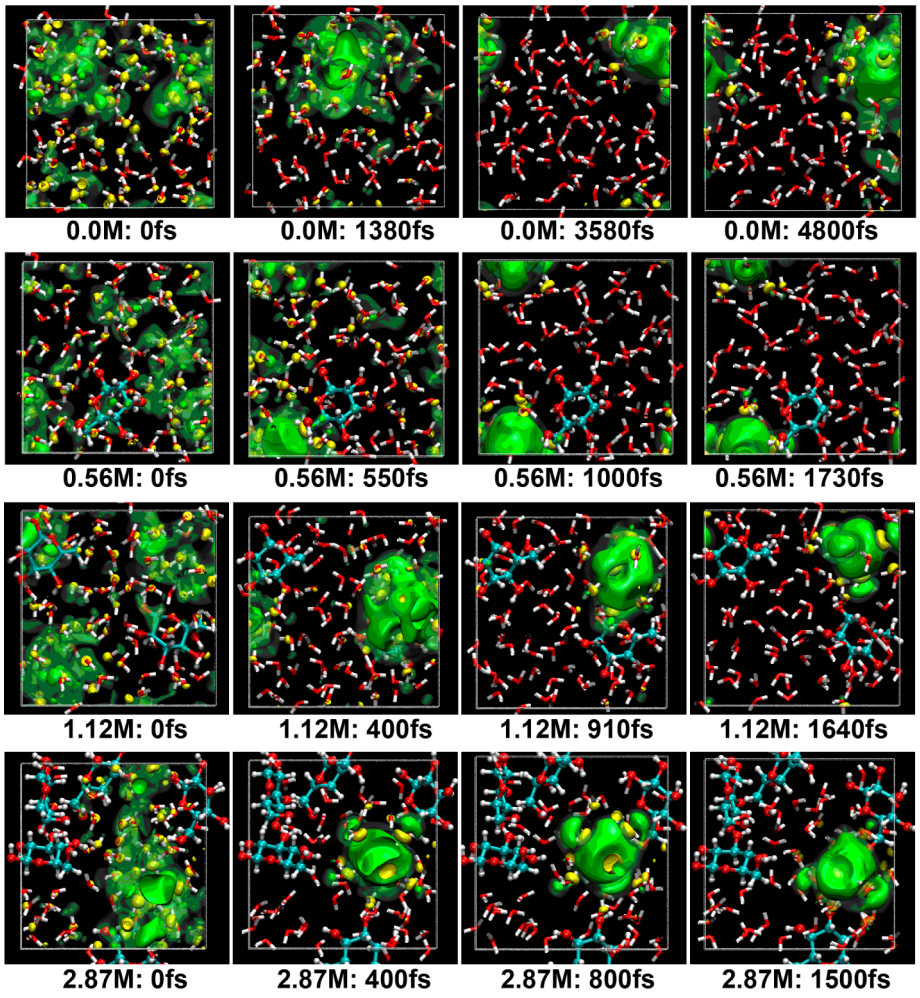

Figure 1. Time evolution of a vertically injected 0 eV EE in the 0.0, 0.56, 1.12, and 2.87 M AGSs. The green and yellow opaque shades denote the negative and positive parts of the singly occupied Kohn−Sham orbital (isovalue = 0.018), respectively, while the corresponding lime transparent shades are the orbital at the isovalue of 0.01. When the orbital isovalue decreases, the shape of the cavity-shaped localized hydrated EE is slightly enlarged.

characteristics suggest the possibility for structural arrest of an EE in a void around a glucose molecule and guarantee that a glucose molecule is not a deep electron trap or scavenger in solution.

Moreover, the hydrated glucoses play important role in biological processes.[29,30] Photoirradiation can generate many secondary electrons, which then transport, or are captured, in such glucose-containing media, as also observed in DNA or protein solutions. Unraveling interactions of an EE with the composite molecules of biological media including water, glucose solutions, and others, and their migration mechanisms, is important for the understanding of numerous biological processes. However, although the relative stability of various rotational conformers of a glucose molecule, and the structural, dynamic and static properties of an AGS have been extensively investigated,[38−45] information about electron solvation in AGSs is scarce and poorly understood.

Here, we report an ab initio molecular dynamics (AIMD) simulation study of the dynamics of an EE in different AGSs with a particular emphasis on the role of glucose molecules in efficiently localizing an injected EE. We show that introduction of glucose(s) not only can considerably reduce the localization time of a vertically injected EE but also effectively compacts and tethers the formed solvated electron cavity. Moreover, the localization efficiency is proportional to the AGS concentration. We find that the localization is in the vicinity of glucose molecule(s), and the solvation cavity consists mainly of water molecules, with the glucose molecules playing an assisting role as a scaffold to tether the solvation cavity, or as a stabilizer to maintain the cavity structure through single −OH participation in forming the cavity. As an essential aspect, this study proves that glucose molecules can considerably enhance localization efficiency of an EE in an AGS, featuring a shortened initial localization time and a compacted cavity-shaped structure compared with these properties in water.

2. CALCULATIONAL AND SIMULATION METHODS

AIMD simulations were performed for the electron injected AGS systems at 300 K with glucose concentrations of 0.0, 0.56, 1.12, and 2.87 M, which are modeled by $(\text{glucose})_n + (H_2O)_m$ in a cubic box (Supporting Information Table S1), respectively. The periodically repeated box was equilibrated in the canonical ensemble (NVT) using the CP2K/Quickstep package.[46] The system was first equilibrated by a 8.0 ns classical molecular dynamics simulation. After further equilibration for 3.0 ps using AIMD simulation, one excess electron was added and another 5.0 ps AIMD simulation was carried out. Electronic structure calculations are based on the Kohn−Sham formulation of the

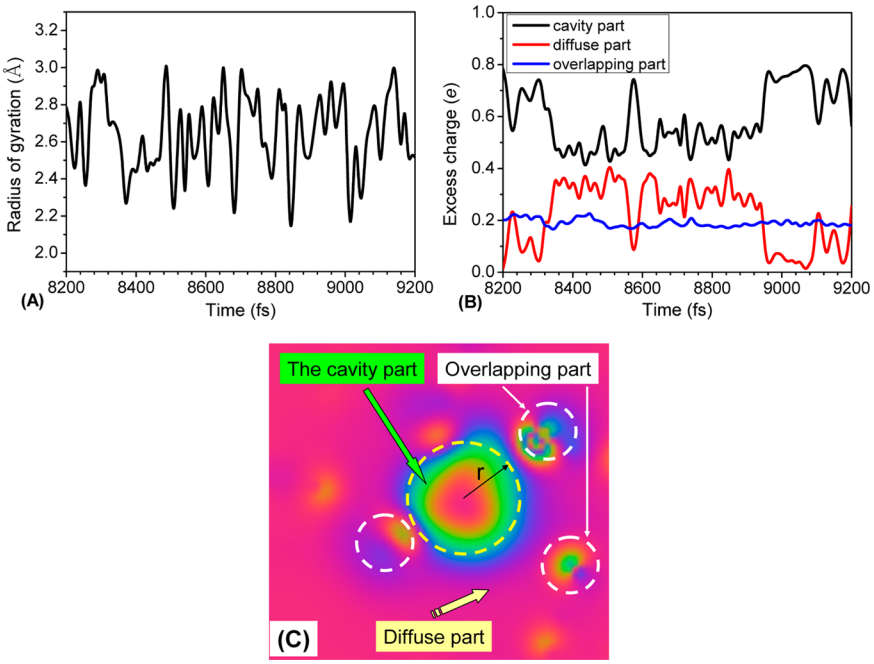

Figure 2. (A) Time evolution of the radius of gyration (r_g) of the EE in water for an arbitrary 1 ps time interval (8.2−9.2 ps). (B) Populations of the EE charge over three regions: (i) the cavity part residing within a 2.5 Å (the approximately average r_g) radius of the center of the hydrated electron (black-solid line, nonvalence part); (ii) the diffuse nonvalence part permeating the hydrogen-bonding network (red-dash line); (iii) the valence part localizing at H_2O molecules (blue-dot line, also the overlapping part with atom positions). (C) A slice of a well-structured solvated EE (cavity-like, localized) shown by the singly occupied Kohn−Sham orbitals. The blue-green color denotes larger value, while the red color denotes smaller value. The yellow dash circle is the cavity part, while the white dash circle is the overlapping part (covalent part). The other region outside the cavity is the diffuse part.

density functional theory (DFT) employing a hybrid Gaussian and plane wave (GPW) method. The Becke, Lee, Yang, and Parr (BLYP)[47,48] exchange-correlation functional with the empirical dispersion correction[49] was used, which predicts properties of liquid water reasonably well.[50] The Kohn−Sham orbitals were expanded into a triple-ζ valence basis set augmented with two sets of *d*-type or *p*-type polarization functions (TZV2P). An auxiliary plane wave basis set with a cutoff of 300 Ry was used to describe the valence electrons. The core electrons were removed by the introduction of norm-conserving pseudopotentials developed by Goedecker, Teter, and Hutter (GTH).[51,52] Self-consistent field calculations were done with a convergence criterion of 10^{-6} Hartree on the total energy. The time step was set to 0.5 fs and the temperature was controlled by a Nosé−Hoover chain thermostat.[53] The self-interaction error of DFT was corrected for by introducing a self-interaction correction (SIC) method within a restricted open shell Kohn−Sham scheme.[54] The accuracy of the BLYP functional and TZV2P basis set was checked by comparing additional trajectories obtained at the PBE/TZV2P and BLYP/*m*-TZV2P[55] levels, respectively. This simulation scheme is similar to that extensively used in literatures and has been probed to be suitable method.[4−6] The relevant results are given below from which consistency of our simulation results is verified.

Optical adsorption spectra were calculated by exciting hydrated electron from the ground electronic state to first seven excited states. The time-dependent density functional theory (TDDFT)[56] was performed through the CASTEP package available from Accelrys Inc. Energy and forces are evaluated with the PBE exchange-correlation function and ultrasoft pseudopotentials. The energy cutoff was set 300 eV. Gamma points were used to integrate the wave function in reciprocal space. Self-consistent field calculations were done with a convergence criterion of 2×10^{-6} Hartree on the total energy. The TDDFT calculations were based on the single-point calculations for the single snapshot extracted from the CP2K simulation trajectory. The periodic boundary conditions were applied: (i) for the AGS solutions, the single snapshot configuration that was placed in a cubic box with a length of 14.41 Å (0.0 M), 14.41 Å (0.56 M), 14.36 Å (1.12 M), or 14.24 Å (2.87 M); (ii) for the $(H_2O)^-_{50}$ cluster, the single snapshot configuration that was placed in a cubic box with a length of 22 Å.

In addition, to clarify the size effect and the equilibration case of the system, we perform additional AIMD simulations using large unit cells and the relevant parameters are shown in Supporting Information Table S2. The system is equilibrated for 8 ns at the classical MD level and then for 5 ps at the AIMD level. After adding an EE vertically, the trajectory is recorded along the evolution time for 2 ps. The relevant results are given in the Supporting Information, which reproduces our observed phenomena and confirms our conclusions.

3. RESULTS AND DISCUSSION

Excess Electron in Water. To establish a benchmark for comparison, and as a starting point, we first AIMD simulated an EE solvation in water. As expected, due to the strong H-bonding network and the absence of preexisting traps for EE localization, upon injection, an EE first occupies the water conduction band as a diffuse presolvated state. Figure 1 illustrates this state by plotting the singly occupied Kohn−Sham orbital, which is seen to extend over a large region. This diffuse conduction band state lasts for several hundreds of

dx.doi.org/10.1021/ct500238k | J. Chem. Theory Comput. 2014, 10, 4189−4197

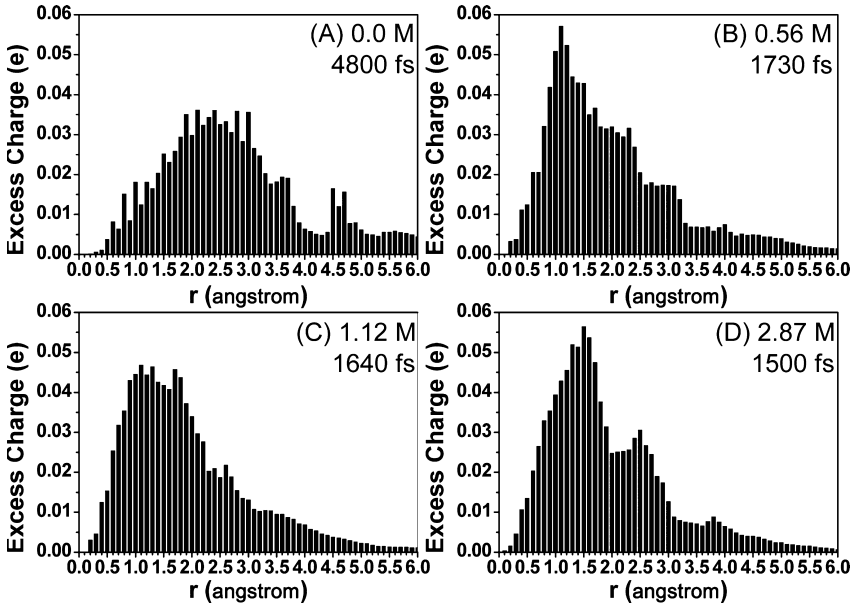

Figure 3. Distribution of EE in each spherical shell (Δr = 0.1 Å) at r from the center of the cavity-shaped solvated EE in water and three AGSs. The total EE charges within a 5.0 Å radius of the center of the solvated EE cavity are ∼0.89 e and ∼0.96 e for water and three AGSs, respectively.

femtoseconds and then starts to exhibit a localization propensity. After ∼1.5 ps, the EE becomes localized in a cavity-shaped solvated state (Figure 1) arising from the requirements of breaking the strong H-bonding network and the reorganization of the local water structure. However, this cavity-shaped state is not a conventional cavity-trapped state for most of the time evolution. In this cavity-shaped state, a considerable part of the EE resides outside the cavity and permeates the H-bonding network of its surrounding solvation shell.

Given that this state is different from those found in several previous models,[26−28] we extended the AIMD simulation by another 5.0 ps and monitored variations of the EE radius of gyration (r_g) and its distribution (Figure 2). As shown in Figure 2(A), r_g fluctuates around its average value of ∼2.6 Å, which is in reasonable agreement with the experimental estimate.[57,58] To characterize the structure of the hydrated EE, we divided the EE charge into three parts,[28] as illustrated in Figure 2(C): (i) the charge enclosed in a cavity of radius 2.5 Å (the cavity part); (ii) the charge permeating the H-bonding network (the diffuse, nonvalence part); (iii) the charge localizing at more water molecules by occupying their valence orbitals, thus overlapping with atom positions (the valence part). The time evolutions of these three parts of the EE charge are plotted in Figure 2(B), which reveals charge exchanges or redistributions among the three regions. Interestingly, the cavity part contains 40−60% of the total EE charge, and sometimes may reach ∼80%, while the overlapping valence part is an essentially constant 20%. The transfers of charge occur between the cavity and diffuse parts during the time evolution, with these two nonvalence parts amounting to ∼80% of the EE. This observation matches closely with literature results obtained by a very different methodology.[59] Furthermore, the localized EE exhibits s-type character, and its radial distribution is Gaussian-like, with a peak at ∼2.5 Å, and a long tail (Figure 3A), as also evidenced by its $4\pi r^2$-multiplied spin density radial distribution as a function of the distance (r) from the center of the excess electron (Supporting Information Figure S12). The spatial region further out from the radius 2.5 Å shell also exhibits considerable EE density, which approximately corresponds to the summation of the diffuse and valent parts. In addition, the calculated vertical detachment energies (VDEs) of the fully hydrated EE are in the range 2.9−3.2 eV with an average value of ∼3.1 eV (Supporting Information Figure S20), which is in reasonable agreement with the corresponding experimental value (3.3 eV).[7f]

Further verification of these results using different simulation methods and system sizes support our conclusions (Supporting Information Figures S3−S4 and S16−S20). All these results are consistent with experiments[57,58] and with other theoretical methods[27,28,59] and makes us confident that the AIMD simulation method employed here is reliable.

Structures of Solvated EE in AGSs. With these results in hand, we monitored the behavior of an EE in a 0.56 M AGS modeled by a system containing one glucose and 90 H_2O molecules in a cubic cell with a side of 14.41 Å. Similar to that in water, the injected EE occupies the bottom of the conduction band as a slightly diffuse state. As expected,[37] the glucose molecule basically does not participate in binding the EE in the early time evolution, even though it has five hydroxyls (−OH) linked to a relatively rigid pyrane ring. This observation can be attributed to the following: (1) The formation of intramolecular H-bonds weakens the ability of glucose to bind an EE. (2) Although the lowest unoccupied molecular orbital energy level of a glucose molecule is lower than that of a water molecule, it is considerably higher than the bottom of the liquid water conduction band. The conduction band bottom of AGS still consists of the lowest unoccupied molecular orbitals of H_2O molecules. (3) Although hydration increases the dipole moment of a glucose molecule from 2.95 to 3.27 D, the polarity of a hydrated glucose is still too weak to bind an EE. (4) Glucose has two hydrophobic zones, above and below the six-membered pyrane ring, that also are not favorable to electron binding. Clearly, the glucose molecule is not a deep trap for an EE. It only plays an assisting role in capturing the injected dry EE in this dilute AGS. We further examined the structure and dynamics of the bound EE. The results indicate that it gradually converts from the slightly diffuse conduction band dry state to a

dx.doi.org/10.1021/ct500238k | J. Chem. Theory Comput. 2014, 10, 4189−4197

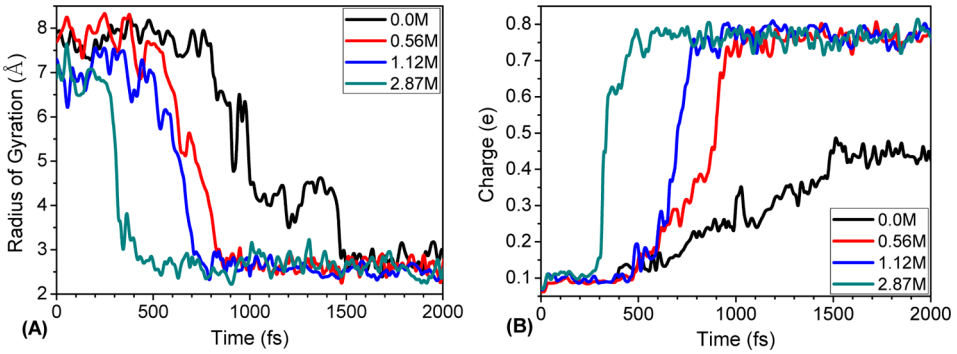

Figure 4. Time evolutions of the radius of gyration (r_g) of the EE (A) and the EE charge residing within a 2.5 Å radius of the center of the solvated EE (B) in the 0.0, 0.56, 1.12, and 2.87 M AGSs.

cavity-shaped localized solvated state, as shown in Figure 1. The solvent cavity consists of a −OH group of glucose and 3 H_2O molecules (a tetrameric cavity). The localization time is only ∼0.8 ps, which is considerably shorter than that (∼1.5 ps) in water. The localized EE does not escape from the solvent cavity in the subsequent time evolution and does not convert to any diffuse states.

To examine the cooperativity of two glucose molecules in binding an EE in AGS, two glucose molecules were added into a cubic cell of 85 H_2O molecules, with a side of 14.36 Å, resulting in 1.12 M AGS. A similar picture was observed, whereby a vertically added EE occupies the conduction band bottom as a slightly diffuse conduction band state, and the two glucose molecules basically do not participate in binding the EE in the early evolution. We particularly checked the localized structure of the solvated EE and found that only one glucose molecule participates in forming the solvation cavity (Figure 1). This observation again indicates that a glucose molecule is not a deep EE trap in condensed media, as also supported indirectly by the experimental observations that EEs are trapped intermolecularly in glucose crystals, forming solvated EEs instead of valence anions.[31−35] In addition, the localization time is ∼0.6 ps, which is shorter than those (1.5 and 0.8 ps) in both water and 0.56 M AGS. Also, the localized EE is always trapped in a cavity for the duration of the simulation.

A dense AGS (2.87 M) was also considered, which corresponds to a mixture of 5 glucose and 60 H_2O molecules in a cubic cell with a side of 14.24 Å. As expected, the initial localization time becomes much shorter (only ∼0.3 ps), and also, once formed, the localized EE does not move out of the cavity over the course of the AIMD simulation. This solvated EE is confined in a pocket formed by 3−4 glucose molecules, and the solvation cavity of the EE consists of 3 H_2O molecules and 1 glucose −OH group (Figure 1), similar to those observed above. The trapping mode observed here is in agreement with intermolecular trapping in glucose crystals.[31−35] However, the solvation cavity for the EE is dynamical, instead of rigid as in a crystal, and ligand exchange and a slight distortion of the solvent shell in the pocket occasionally occurs in the time evolution.

As a comparison with water, the structures of the localized, cavity-shaped solvated EEs in the AGSs were also evaluated. The calculated r_g of the localized solvated EEs in the three AGSs are ∼2.5 Å, almost equivalent to that in water. However, the EE distributions of the localized solvated EEs in the three AGSs are considerably different from that in water, as shown in Figure 3. The radial distributions in a solvated EE cavity in any of the AGSs exhibit a non-Gaussian character, with a peak at ∼1.1 Å. The peak not only tends to be higher but is definitely shifted toward the center of the cavity, compared with that in water. Thus, the solvated EE cavity is considerably reduced and compacted in the AGSs relative to water.

In addition, we calculated the average optical absorption spectrum and the density of states from the snapshots of the simulation (Supporting Information Figure S7). The ground-state absorption spectra that originate from the transition from the singly occupied Kohn−Sham orbital to the lowest seven unoccupied orbitals for each case were calculated using the TD-DFT method.[56] The spectra of an EE in the 0.0, 0.56, 1.12, and 2.87 M AGSs are similar to each other with the peaks located at 1.5−1.6 eV (Supporting Information Figure S7), but the peaks of the spectra blue-shift along with the increase of the glucose concentration. This peak value is lower by 0.1 eV than the experimental one for the hydrated EE in water most likely because only a finite number of excited states were accounted for in the calculations. These results closely match the experimental ones for hydrated electrons.[57,58] This high degree of agreement also indicates that the localized EE in an AGS is in a cavity-shaped hydrated electron state, or at least has a similar property to the hydrated electron in water. Addition of different amounts of glucose molecules into water results in little change of the solution energy gap, which is in agreement with the calculated electronic spectra of the EE in AGSs (Supporting Information Figure S7).

As an additional energy indicator of the solvated electrons formed in such solutions, the vertical detachment energies of the fully solvated electrons were also calculated. The localized EEs in three aqueous glucose solutions have similar but slightly larger VDE values (3.2−3.4 eV) than those in water (Supporting Information Figure S20). This observation indicates that the localized EE in glucose solutions are slightly more compacted. This conclusion is also in good agreement with the electron cloud distribution variations.

Evolution Dynamics. To further characterize the localization dynamics of an EE in such solutions, we survey the relevant AIMD simulation results of the above-mentioned four situations (0.0, 0.56, 1.12, and 2.87 M AGSs) and find that introducing glucose molecules into water, or increasing the glucose concentration in an AGS, can significantly shorten the time to localize the injected dry EE and more efficiently localize the EE into a solvent cavity, compared with that of an EE in pure water. First, we monitored the variations of the radii of gyration, as displayed in Figure 4(A) for a 5 ps time interval. In pure water, r_g is very large (∼8 Å) in the initial ∼1.0 ps and

dx.doi.org/10.1021/ct500238k | J. Chem. Theory Comput. 2014, 10, 4189−4197

then reaches its final value of ∼2.5 Å in the subsequent 0.5 ps. For the 0.56, 1.12, and 2.87 M AGSs, an EE acquires its final radius of gyration (∼2.5 Å) in ∼0.8, ∼0.6, and ∼0.3 ps, respectively, agreeing well with the above-mentioned localization times derived from the time evolution of the orbital variations. These almost equivalent equilibrium values of r_g in the four solutions all are very close to the experimental estimate for a hydrated electron in water,[57,58] again indicating that after localization the injected EE in these hydroxyl-containing solutions is trapped in a cavity as a hydrated electron. We also calculated the cavity-enclosed partial EE charges, as shown in Figure 4B. Generally, when an EE is well localized in a cavity, the in-cavity part amounts to roughly 80% of the total charge.[59] However, in the time evolution process, a part of the EE cloud can permeate the H-bonding network, leading to a decrease in the amount of charge in the cavity. In such a slightly diffuse state, the EE prefers to distribute over a large region, and its population in a 2.5 Å radius of the EE center is relatively small. Thus, for an EE in pure water, the flat part in Figure 4B could be a feature that an EE is in a slightly loose cavity. In this figure, in the 0.5−1.5 ps time region, the charge of the cavity part gradually increases and reaches a value of ∼0.42 e. This time scale and that of r_g are in good agreement and thus also reflects the localization time. In contrast, accelerated evolution processes are observed in all three AGSs but with different rates. Furthermore, the cavity charge reaches a value of ∼0.80 e and remains unchanged in the subsequent time evolution (Supporting Information Figure S10). Figure 5 presents a

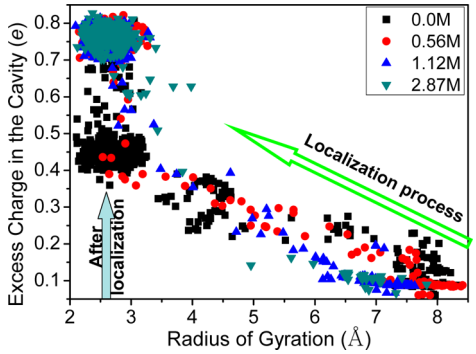

Figure 5. Correlation of the EE charge residing in the hydration cavity (the cavity part) with the radius of gyration of the solvated EE in water and the three AGSs observed in the simulations.

correlation of the cavity part charge with r_g of a solvated EE. Clearly, during the localization process, there is a good linear correlation. After localization, the r_g of a solvated electron in the four systems remain unchanged, with values 2.0−3.0 Å and average ∼2.5 Å. However, the cavity part charge maintains ∼70−80% of the EE in the three AGSs, while it is only ∼40−50% in water for most of the time, with an occasional increase up to ∼80%. The contraction process and distribution characteristics of the EE cloud can be also well understood by calculating the EE charges in each spherical shell (Δr = 0.1 Å) at r from the center of the solvated electron, for the different snapshot configurations in the AGS (Supporting Information Figure S13).

To examine how glucose molecules participate in binding the EE, and form the localized solvation cavity, the distances between the center of the injected EE and nearby H atoms of glucose molecules are shown in Figure 6. This indicates that the

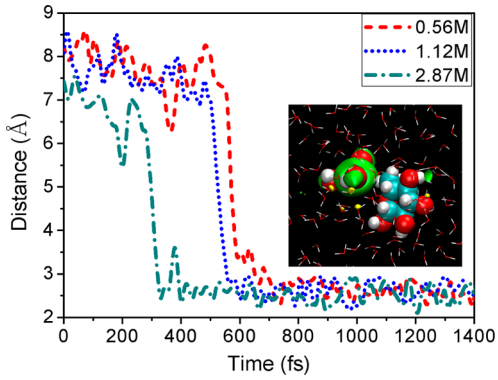

Figure 6. Time evolution of the distance between the center of the solvated EE and a −OH hydrogen of a glucose that participates in forming a solvation cavity in the 0.56, 1.12, and 2.87 M AGSs. The inset shows a typical cavity structure of the solvated EE consisting of three water molecules and one −OH of a glucose molecule (shown in VDW model).

EE localization takes place in the vicinity of glucoses, and a glucose −OH participates in forming a solvent cavity to accommodate the EE. In detail, (i) participation of glucose in binding the EE is not synchronous with the formation of the solvated EE cavity; (ii) in the glucose-formed pocket, the EE is first captured by a glucose in a Rydberg state and then is hydrated, forming a tetrameric cavity-shaped hydrated state (Figure 6); (iii) ligand exchange occurs among water molecules, and at least one of the glucose molecules always participates in constructing the solvation cavity in the ligand exchange process.

The presence of glucose can inhibit the mobility of water molecules[44] and further affect the diffusion dynamics of AGSs. The defective H-bonding network in such AGSs can reasonably explain the shortening of the initial localization times and rationalize the cavity-trapped states in AGSs with respect to those in water. In the initial localization process, because electron localization needs to first break the strong H-bonding network in water, and thermal-fluctuation-induced random motion of water molecules also does not favor the formation of a solvation cavity, localization requires a long time in water (e.g., ∼1.5 ps in the present AIMD simulation). However, although a glucose molecule is not a strong electron captor or attractor and does not have the ability to trap an EE, it can inhibit the mobility of water molecules around it in an AGS,[44] as revealed by the reduced diffusion coefficients in the AGSs (Supporting Information Figure S14) relative to that in liquid water, and thus forces such water molecules to reorient in the vicinity of glucose molecules to create a cavity for stabilizing the injected dry EE. In addition, the existence of glucose molecules breaks the local H-bonded network, leading to small voids, freeing glucose −OH hydrogens around glucose molecules. As a result, the water molecules around glucose(s) are relatively free and have a larger reorientational freedom than those in a pure water region, as evidenced by faster decays of the rotational time correlation functions of the water molecules around the glucose molecule than those of the water molecules apart from the glucose (Supporting Information Figure S15). Therefore, an EE is more readily localized in an AGS compared to that in pure water, and the higher the concentration of glucose, the faster the localization of an EE in solution.

dx.doi.org/10.1021/ct500238k | J. Chem. Theory Comput. 2014, 10, 4189−4197

4. CONCLUSIONS

In summary, we studied the structure and the dynamics of an EE in different concentration AGSs using AIMD simulations. The main finding is that introduction of glucose molecules into water considerably shortens the localization time and better localizes the EE in a cavity compared with the cavity in water, with the variation in localization time depending strongly on the glucose concentration. In particular, in water just 40−60% of an EE resides in a cavity, while in the AGSs the cavity amounts to ∼80% of a solvated electron. The glucose molecules play an assisting role as cavity promoters, through generating a preexisting void for an EE to reside in, and as a stabilizer, through tethering the formed solvation cavity in the solvation and evolution processes. An important implication of this work is that it provides a new strategy to efficiently localize EEs as cavity-shaped solvated electrons using the highly soluble saccharide-like or polyhydroxyl molecules as promoters and stabilizers.

It should be noted that the present work provides adiabatic dynamics information from the well-modeled systems, which can be applied to many important processes; however, a lot of relevant electron solvation processes possess nonadiabatic characters and thus require explorations at the nonadiabatic level. Clearly, further nonadiabatic dynamics studies on more realistic processes are needed. Besides, it is also important to improve the samplings of more trajectories to obtain more quantitative descriptions on the localization dynamics.

■ ASSOCIATED CONTENT

Supporting Information

Calculational and simulation methods; molecular structures and relevant properties of α-glucose and β-glucose; reviewing properties of anionic water clusters; additional AIMD simulation results for an EE in water; calculations of charge partition in three regions; radial distributions of solvated EEs in water and AGSs and its time evolutions; the calculated MSD and diffusion coefficients; etc. This material is available free of charge via the Internet at http://pubs.acs.org.

■ AUTHOR INFORMATION

Corresponding Author

*Email: byx@sdu.edu.cn.

Notes

The authors declare no competing financial interest.

■ ACKNOWLEDGMENTS

This work was supported by NSFC (21373123, 20633060, and 20973101), NSF (ZR2013BM027) of Shandong Province. A part of the calculations were carried out at National Supercomputer Center in Jinan, Shanghai Supercomputer Center, and High-Performance Supercomputer Center at SDU-Chem.

■ REFERENCES

(1) Young, R. M.; Neumark, D. M. Dynamics of Solvated Electrons in Clusters. *Chem. Rev.* **2012**, *112*, 5553−5577. Bragg, A. E.; Verlet, J. R. R.; Kammrath, A.; Cheshnovsky, O.; Neumark, D. M. Hydrated Electron Dynamics: From Clusters to Bulk. *Science* **2004**, *306*, 669−671. Paik, D. H.; Lee, I. R.; Yang, D. S.; Baskin, J. S.; Zewail, A. H. Electrons in Finite-Sized Water Cavities: Hydration Dynamics Observed in Real Time. *Science* **2004**, *306*, 672−675. Bragg, A. E.; Verlet, J. R. R.; Kammrath, A.; Cheshnovsky, O.; Neumark, D. M. Electronic Relaxation Dynamics of Water Cluster Anions. *J. Am. Chem. Soc.* **2005**, *127*, 15283−15295. Shreve, A. T.; Elkins, M. H.; Neumark, D. M. Photoelectron Spectroscopy of Solvated Electrons in Alcohol and Acetonitrile Microjets. *Chem. Sci.* **2013**, *4*, 1633−1639. Ehrler, O.; Neumark, D. M. Dynamics of Electron Solvation in Molecular Clusters. *Acc. Chem. Res.* **2009**, *42*, 769−777. Sommerfeld, T.; Jordan, K. D. Electron Binding Motifs of $(H_2O)_n^-$ Clusters. *J. Am. Chem. Soc.* **2006**, *128*, 5828−5833. Aitken, F.; Li, Z.-L.; Bonifaci, N.; Denat, A.; von Haeften, K. Electron Mobility in Liquid and Supercritical Helium Measured Using Corona Discharges: A New Semi-Empirical Model for Cavity Formation. *Phys. Chem. Chem. Phys.* **2011**, *13*, 719−724.

(2) Herbert, J. M.; Head-Gordon, M. Charge Penetration and the Origin of Large O−H Vibrational Red-Shifts in Hydrated-Electron Clusters, $(H_2O)_n^-$. *J. Am. Chem. Soc.* **2006**, *128*, 13932−13939. Jacobson, L. D.; Herbert, J. M. A One-Electron Model for the Aqueous Electron That Includes Many-Body Electron-Water Polarization: Bulk Equilibrium Structure, Vertical Electron Binding Energy, and Optical Absorption Spectrum. *J. Chem. Phys.* **2010**, *133*, 154106. Jacobson, L. D.; Herbert, J. M. Polarization-Bound Quasi-Continuum States Are Responsible for the "Blue Tail" in the Optical Absorption Spectrum of the Aqueous Electron. *J. Am. Chem. Soc.* **2010**, *132*, 10000−10002. Herbert, J. M.; Head-Gordon, M. First-Principles, Quantum-Mechanical Simulations of Electron Solvation by a Water Cluster. *Proc. Natl. Acad. Sci. U.S.A.* **2006**, *103*, 14282−14287. Herbert, J. M.; Jacobson, L. D. Structure of the Aqueous Electron: Assessment of One-Electron Pseudopotential Models in Comparison to Experimental Data and Time-Dependent Density Functional Theory. *J. Phys. Chem. A* **2011**, *115*, 14470−14483. Jacobson, L. D.; Herbert, J. M. Theoretical Characterization of Four Distinct Isomer Types in Hydrated-Electron Clusters, and Proposed Assignments for Photoelectron Spectra of Water Cluster Anions. *J. Am. Chem. Soc.* **2011**, *133*, 19889−19899. Herbert, J. M.; Jacobson, L. D. Nature's Most Squishy Ion: The Important Role of Solvent Polarization in the Description of the Hydrated Electron. *Int. Rev. Phys. Chem.* **2011**, *30*, 1−48. Jacobson, L. D.; Herbert, J. M. A One-Electron Model for the Aqueous Electron that Includes Many-Body Electron−Water Polarization: Bulk Equilibrium Structure, Vertical Electron Binding Energy, and Optical Absorption Spectrum. *J. Chem. Phys.* **2010**, *133*, 154506. Barnett, R. N.; Landman, U.; Cleveland, C. L.; Jortner, J. Electron Localization in Water Clusters. 1. Electron−Water Pseudopotential. *J. Chem. Phys.* **1988**, *88*, 4421−4428. Barnett, R. N.; Landman, U.; Cleveland, C. L. Electron Localization in Water Clusters. II. Surface and Internal States. *J. Chem. Phys.* **1988**, *88*, 4429−4447.

(3) Turi, L.; Sheu, W. S.; Rossky, P. J. Characterization of Excess Electrons in Water-Cluster Anions by Quantum Simulations. *Science* **2005**, *309*, 914−917. Turi, L.; Rossky, P. J. Theoretical Studies of Spectroscopy and Dynamics of Hydrated Electrons. *Chem. Rev.* **2012**, *112*, 5641−5674. Madarász, Á.; Rossky, P. J.; Turi, L. Response of Observables for Cold Anionic Water Clusters to Cluster Thermal History. *J. Phys. Chem. A* **2010**, *114*, 2331−2337. Wong, K. F.; Rossky, P. J. Mean-Field Molecular Dynamics with Surface Hopping: Application to the Aqueous Solvated Electron. *J. Phys. Chem. A* **2001**, *105*, 2546−2556.

(4) Wang, Z. P.; Liu, J. X.; Zhang, M.; Cukier, R. I.; Bu, Y. X. Solvation and Evolution Dynamics of an Excess Electron in Supercritical CO_2. *Phys. Rev. Lett.* **2012**, *108*, 207601. Liu, J. X.; Wang, Z. P.; Zhang, M.; Cukier, R. I.; Bu, Y. X. Excess Dielectron in an Ionic Liquid as a Dynamic Bipolaron. *Phys. Rev. Lett.* **2013**, *110*, 107602. Liu, J. X.; Cukier, R. I.; Bu, Y. X. Bending Vibration-Governed Solvation Dynamics of an Excess Electron in Liquid Acetonitrile Revealed by Ab Initio Molecular Dynamics Simulation. *J. Chem. Theory Comput.* **2013**, *9*, 4727−4734.

(5) Wang, Z. P.; Zhang, L.; Chen, X. H.; Cukier, R. I.; Bu, Y. X. Excess Electron Solvation in an Imidazolium-Based Room-Temperature Ionic Liquid Revealed by Ab Initio Molecular Dynamics Simulations. *J. Phys. Chem. B* **2009**, *113*, 8222−8226. Wang, Z. P.; Zhang, L.; Cukier, R. I.; Bu, Y. X. States and Migration of an Excess Electron in a Pyridinium-Based, Room-Temperature Ionic Liquid: An Ab Initio Molecular Dynamics Simulation Exploration. *Phys. Chem. Chem. Phys.* **2010**, *12*, 1854−1861.

(6) Marsalek, O.; Uhlig, F.; VandeVondele, J.; Jungwirth, P. Structure, Dynamics, and Reactivity of Hydrated Electrons by Ab Initio Molecular Dynamics. *Acc. Chem. Res.* **2012**, *45*, 23−32. Frigato, T.; VandeVondele, J.; Schmidt, B.; Schutte, C.; Jungwirth, P. Ab Initio Molecular Dynamics Simulation of a Medium-Sized Water Cluster Anion: From an Interior to a Surface-Located Excess Electron via a Delocalized State. *J. Phys. Chem. A* **2008**, *112*, 6125−6133. Uhlig, F.; Marsalek, O.; Jungwirth, P. Electron at the Surface of Water: Dehydrated or Not? *J. Phys. Chem. Lett.* **2013**, *4*, 338−343. Marsalek, O.; Uhlig, F.; Jungwirth, P. Electrons in Cold Water Clusters: An Ab Initio Molecular Dynamics Study of Localization and Metastable States. *J. Phys. Chem. C* **2010**, *114*, 20489−20495.

(7) (a) Casey, J. R.; Larsen, R. E.; Schwartz, B. J. Resonance Raman and Temperature-Dependent Electronic Absorption Spectra of Cavity and Noncavity Models of the Hydrated Electron. *Proc. Natl. Acad. Sci. U.S.A.* **2013**, *110*, 2712−2717. (b) Casey, J. R.; Kahros, A.; Schwartz, B. J. To Be or Not to Be in a Cavity: The Hydrated Electron Dilemma. *J. Phys. Chem. B* **2013**, *117*, 14173−14182. (c) Laenen, R.; Roth, T.; Laubereau, A. Novel Precursors of Solvated Electrons in Water: Evidence for a Charge Transfer Process. *Phys. Rev. Lett.* **2000**, *85*, 50−53. (d) Silva, C.; Walhout, P. K.; Yokoyama, K.; Barbara, P. F. Femtosecond Solvation Dynamics of the Hydrated Electron. *Phys. Rev. Lett.* **1998**, *80*, 1086−1089. (f) Siefermann, K. R.; Liu, Y.; Lugovoy, E.; Link, O.; Faubel, M.; Buck, U.; Winter, B.; Abel, B. Binding Energies, Lifetime, and Implications of Bulk and Interface Solvated Electrons in Water. *Nat. Chem.* **2010**, *2*, 274−279. (g) Migus, A.; Gauduel, Y.; Martin, J. L.; Antonetti, A. Excess Electrons in Liquid Water: First Evidence of a Prehydrated State with Femosecond Lifetime. *Phys. Rev. Lett.* **1987**, *58*, 1559−1562.

(8) Margulis, C. J.; Annapureddy, H. V. R.; De Biase, P. M.; Coker, D.; Kohanoff, J.; Del Pópolo, M. G. Dry Excess Electrons in Room-Temperature Ionic Liquids. *J. Am. Chem. Soc.* **2011**, *133*, 20186−20193. Xu, C.; Durumeric, A.; Kashyap, H. K.; Kohanoff, J.; Margulis, C. J. Dynamics of Excess Electronic Charge in Aliphatic Ionic Liquids Containing the Bis(trifluoromethylsulfonyl)amide Anion. *J. Am. Chem. Soc.* **2013**, *135*, 17528−17536.

(9) Dye, J. L. Electrides: Early Examples of Quantum Confinement. *Acc. Chem. Res.* **2009**, *42*, 1564−1572.

(10) Edwards, P. P. Electrons in Cement. *Science* **2011**, *333*, 49−50.

(11) Kim, S. W.; Shimoyama, T.; Hosono, H. Solvated Electrons in High-Temperature Melts and Glasses of the Room-Temperature Stable Electride $[Ca_{24}Al_{28}O_{64}]^{4+}$ $4e^-$. *Science* **2011**, *333*, 71−74.

(12) Wang, C. R.; Lu, Q. B. Real-Time Observation of a Molecular Reaction Mechanism of Aqueous 5-Halo-2′-Deoxyuridines under UV/Ionizing Radiation. *Angew. Chem., Int. Ed.* **2007**, *46*, 6316−6320.

(13) Sanche, L. Biological Chemistry: Beyond Radical Thinking. *Nature* **2009**, *461*, 358−359.

(14) Wang, C. R.; Nguyen, J.; Lu, Q. B. Bond Breaks of Nucleotides by Dissociative Electron Transfer of Nonequilibrium Prehydrated Electrons: A New Molecular Mechanism for Reductive DNA Damage. *J. Am. Chem. Soc.* **2009**, *131*, 11320−11322.

(15) Wang, C. R.; Lu, Q. B. Molecular Mechanism of the DNA Sequence Selectivity of 5-Halo-2′-Deoxyuridines as Potential Radiosensitizers. *J. Am. Chem. Soc.* **2010**, *132*, 14710−14713.

(16) Matsuishi, S.; et al. High-Density Electron Anions in a Nanoporous Single Crystal: $[Ca_{24}Al_{28}O_{64}]^{4+}(4e^-)$. *Science* **2003**, *301*, 626−629.

(17) Huang, R. H.; Faber, M. K.; Moeggenborg, K. J.; Ward, D. L.; Dye, J. L. Structure of K^+(cryptand[2.2.2J) Electride and Evidence for Trapped Electron Pairs. *Nature* **1988**, *331*, 599−601.

(18) Singh, D. J.; Krakauer, H.; Haas, C.; Pickett, W. E. Theoretical Determination That Electrons Act as Anions in the Electride Cs^+ (15-crown-5)$_2$·e^-. *Nature* **1993**, *365*, 39−42.

(19) Miyakawa, M.; et al. Superconductivity in an Inorganic Electride $12CaO{\cdot}7Al_2O_3{:}e^-$. *J. Am. Chem. Soc.* **2007**, *129*, 7270−7271.

(20) Muhammad, S.; Xu, H.; Liao, Y.; Kan, Y.; Su, Z. Quantum Mechanical Design and Structure of the $Li@B_{10}H_{14}$ Basket with a Remarkably Enhanced Electro-Optical Response. *J. Am. Chem. Soc.* **2009**, *131*, 11833−11840.

(21) Chen, W.; et al. Nonlinear Optical Properties of Alkalides Li^+(calix[4]pyrrole)M^- (M = Li, Na, and K): Alkali Anion Atomic Number Dependence. *J. Am. Chem. Soc.* **2006**, *128*, 1072−1073.

(22) Xu, H. L.; et al. Structures and Large NLO Responses of New Electrides: Li-Doped Fluorocarbon Chain. *J. Am. Chem. Soc.* **2007**, *129*, 2967−2970.

(23) Simon, S. H. A Sound (and Light) Way to Measure Confined Electrons. *Science* **2009**, *324*, 1022−1023.

(24) Kukushkin, I. V.; Smet, J. H.; Scarola, V. W.; Umansky, V.; von Klitzing, K. Dispersion of the Excitations of Fractional Quantum Hall States. *Science* **2009**, *324*, 1044−1047.

(25) Michael, B. D.; O'Neill, P. A Sting in the Tail of Electron Tracks. *Science* **2000**, *287*, 1603−1604.

(26) Boero, M.; Parrinello, M.; Terakura, K.; Ikeshoji, T.; Liew, C. C. First-Principles Molecular-Dynamics Simulations of a Hydrated Electron in Normal and Supercritical Water. *Phys. Rev. Lett.* **2003**, *90*, 226403. Boero, M. Excess Electron in Water at Different Thermodynamic Conditions. *J. Phys. Chem. A* **2007**, *111*, 12248−12256.

(27) Larsen, R. E.; Glover, W. J.; Schwartz, B. J. Does the Hydrated Electron Occupy a Cavity? *Science* **2010**, *329*, 65−69. Jacobson, L. D.; Herbert, J. M. Comment on "does the hydrated electron occupy a cavity? *Science* **2011**, *331*, 1387. Turi, L.; Madarász, Á. Comment on "does the hydrated electron occupy a cavity? *Science* **2011**, *331*, 1387. Larsen, R. E.; Glover, W. J.; Schwartz, B. J. Response to comments on "does the hydrated electron occupy a cavity? *Science* **2011**, *331*, 1387.

(28) Uhlig, F.; Marsalek, O.; Jungwirth, P. Unraveling the Complex Nature of the Hydrated Electron. *J. Phys. Chem. Lett.* **2012**, *3*, 3071−3075.

(29) Lemieux, R. U. *Explorations with Sugars: How Sweet It Was*; American Chemical Society: Washington, DC, 1990.

(30) Collins, P. M.; Ferrier, R. J. *Monosaccharides: Their Chemistry and Their Roles in Natural Products*. Wiley: New York, 1995.

(31) Box, H. C.; Budzinski, E. E.; Freund, H. G. Electron Trapping in Irradiated Single Crystals of Organic Compounds. *J. Chem. Phys.* **1978**, *69*, 1309−1311.

(32) Box, H. C.; Budzinski, E. E.; Freund, H. G.; Potter, W. R. Trapped Electrons in Irradiated Single Crystals of Polyhydroxy Compounds. *J. Chem. Phys.* **1979**, *70*, 1320−1325.

(33) Budzinski, E. E.; Potter, W. R.; Potienko, G.; Box, H. C. Characteristics of Trapped Electrons and Electron Traps in Single Crystals. *J. Chem. Phys.* **1979**, *70*, 5040−5044.

(34) Locher, S. E.; Box, H. C. ESR-ENDOR Studies of X-Irradiated Glucose-1-Phosphate Dipotassium Salt. *J. Chem. Phys.* **1980**, *72*, 828−832.

(35) Samskog, P. O.; Kispert, L. D.; Lund, A. Geometric Model of Trapped Electrons in Trehalose Single Crystals X-ray Irradiated at 3 K. An EPR Study. *J. Chem. Phys.* **1983**, *78*, 5790.

(36) Sonoda, M. T.; Skaf, M. S. Carbohydrate Clustering in Aqueous Solutions and the Dynamics of Confined Water. *J. Phys. Chem. B* **2007**, *111*, 11948−11956.

(37) Costa, R. F. D.; Bettega, M. H. F.; Varella, M. T. d. N.; Lima, M. A. P. Electron Collisions with α-D-Glucose and β-D-Glucose Monomers. *J. Chem. Phys.* **2010**, *132*, 124309.

(38) Brady, J. W. Molecular Dynamics Simulations of α-D-Glucose in Aqueous Solution. *J. Chem. Phys.* **1989**, *111*, 5155−5165.

(39) Molteni, C.; Parrinello, M. Glucose in Aqueous Solution by First Principles Molecular Dynamics. *J. Am. Chem. Soc.* **1998**, *120*, 2168−2171.

(40) Lelong, G.; et al. Molecular Dynamics of Confined Glucose Solutions. *J. Chem. Phys.* **2005**, *122*, 164504.

(41) Mason, P. E.; et al. Neutron Diffraction Studies on Aqueous Solutions of Glucose. *J. Chem. Phys.* **2003**, *119*, 3347−3353.

(42) Smith, L. J.; Price, D. L.; Chowdhuri, Z.; Brady, J. W.; Saboungi, M. L. Molecular Dynamics of Glucose in Solution: A Quasielastic Neutron Scattering Study. *J. Chem. Phys.* **2004**, *120*, 3527−3530.

(43) Corchado, J. C.; Sánchez, M. L.; Aguilar, M. A. Theoretical Study of the Relative Stability of Rotational Conformers of α and β-D-

Glucopyranose in Gas Phase and Aqueous Solution. *J. Am. Chem. Soc.* **2004**, *126*, 7311−7319.
(44) Molinero, V.; Goddard, W. A., III Microscopic Mechanism of Water Diffusion in Glucose Glasses. *Phys. Rev. Lett.* **2005**, *95*, 045701.
(45) Mason, P. E.; Neilson, G. W.; Enderby, J. E.; Saboungi, M. L.; Brady, J. W. Structure of Aqueous Glucose Solutions as Determined by Neutron Diffraction with Isotopic Substitution Experiments and Molecular Dynamics Calculations. *J. Phys. Chem. B* **2005**, *109*, 13104−13111.
(46) VandeVondele, J.; Krack, M.; Mohamed, F.; Parrinello, M.; Chassaing, T.; Hutter, J. Quickstep: Fast and Accurate Density Functional Calculations Using a Mixed Gaussian and Plane Waves Approach. *Comput. Phys. Commun.* **2005**, *167*, 103−128.
(47) Becke, A. D. Density-Functional Exchange-Energy Approximation with Correct Asymptotic Behavior. *Phys. Rev. A* **1988**, *38*, 3098.
(48) Lee, C.; Yang, W.; Parr, R. G. Development of the Colle−Salvetti Correlation-Energy Formula into a Functional of the Electron Density. *Phys. Rev. B* **1988**, *37*, 785.
(49) Grimme, S. Semiempirical GGA-Type Density Functional Constructed with a Long-Range Dispersion Correction. *J. Comput. Chem.* **2006**, *27*, 1787−1799.
(50) Lin, I. C.; Seitsonen, A. P.; Tavernelli, I.; Rothlisberger, U. Structure and Dynamics of Liquid Water from Ab Initio Molecular Dynamics—Comparison of BLYP, PBE, and revPBE Density Functionals with and without van der Waals Corrections. *J. Chem. Theory Comput.* **2012**, *8*, 3902−3910.
(51) Goedecker, S.; Teter, M.; Hutter, J. Separable Dual-Space Gaussian Pseudopotentials. *Phys. Rev. B* **1996**, *54*, 1703−1710.
(52) Hartwigsen, C.; Goedecker, S.; Hutter, J. Relativistic Separable Dual-Space Gaussian Pseudopotentials from H to Rn. *Phys. Rev. B* **1998**, *58*, 3641−3662.
(53) Hoover, W. G. Canonical Dynamics: Equilibrium Phase-Space Distributions. *Phys. Rev. A* **1985**, *31*, 1695.
(54) VandeVondele, J.; Sprik, M. A Molecular Dynamics Study of the Hydroxyl Radical in Solution Applying Self-Interaction-Corrected Density Functional Methods. *Phys. Chem. Chem. Phys.* **2005**, *7*, 1363−1367.
(55) VandeVondele, J.; Hutter, J. Gaussian Basis Sets for Accurate Calculations on Molecular Systems in Gas and Condensed Phases. *J. Chem. Phys.* **2007**, *127*, 114105.
(56) Hutter, J. Excited State Nuclear Forces from the Tamm-Dancoff Approximation to Time-Dependent Density Functional Theory within the Plane Wave Basis Set Framework. *J. Chem. Phys.* **2003**, *118*, 3928−3934.
(57) Bartels, D. M.; Takahashi, K.; Cline, J. A.; Marin, T. W.; Jonah, C. D. Pulse Radiolysis of Supercritical Water. 3. Spectrum and Thermodynamics of the Hydrated Electron. *J. Phys. Chem. A* **2005**, *109*, 1299−1307.
(58) Coe, J. V.; Williams, S. M.; Bowen, K. H. Photoelectron Spectra of Hydrated Electron Clusters vs. Cluster Size: Connecting to Bulk. *Int. Rev. Phys. Chem.* **2008**, *27*, 27−51.
(59) Shkrob, I. A.; Glover, W. J.; Larsen, R. E.; Schwartz, B. J. The Structure of the Hydrated Electron. Part 2. A Mixed Quantum/Classical Molecular Dynamics Embedded Cluster Density Functional Theory: Single-Excitation Configuration Interaction Study. *J. Phys. Chem. A* **2007**, *111*, 5232−5243.